COGNITIVE NEUROSCIENCE

Supramodality of neural entrainment: Rhythmic visual stimulation causally enhances auditory working memory performance

Philippe Albouy[1,2,3,4]*, Zaida E. Martinez-Moreno[1,2], Roxane S. Hoyer[4], Robert J. Zatorre[1,2,3]†, Sylvain Baillet[2]†

The frontoparietal network is involved in multiple tasks, such as visual mental rotation, working memory, or arithmetic. Whether those different cognitive processes are supported by the same supramodal network or distinct, but overlapping, functional systems is unresolved. We investigate whether frontoparietal activity can be selectively entrained by rhythmic sensory stimulations (visual rotation) and whether this entrainment can causally modulate task performance in another modality (auditory working memory). We show that rhythmic visual presentations of rotating shapes, known to activate the dorsal pathway, increase frontoparietal connectivity at stimulation frequency as measured with MEG/EEG. We then show that frontoparietal theta oscillations predict auditory working memory performance. Last, we demonstrate that theta rhythmic visual stimulation applied during auditory memory causally enhances performance, and both the rotating properties of the stimulus and its flickering frequency drive the effect. This study provides causal evidence of the supramodal role of the frontoparietal network in human cognition.

INTRODUCTION

The combination of noninvasive brain stimulation procedures with behavioral and brain activity measures has been transformative to cognitive neuroscience research (*1*). In particular, transcranial brain stimulation with simultaneous electrophysiological recordings enables the investigation of causal relationships between brain neurophysiology and cognitive functions (*2*, *3*). This approach consists of using time-resolved measures, such as magnetoencephalography (MEG) or electroencephalography (EEG), to define task-relevant and subject-specific anatomical and electrophysiological properties that inform the noninvasive brain stimulation parameters. Using a similar information-based approach, rhythmic transcranial magnetic stimulation (rh-TMS) or similar techniques can specifically modulate the targeted network and oscillatory neural signals during task performance (*1*, *3*, *4*). Recent studies have shown that rhythmic noninvasive stimulation of supramodal brain regions can enhance higher-order cognitive functions (*5*–*8*). Notably, we previously reported that rh-TMS applied over the intraparietal sulcus (IPS) at the theta frequency (5 Hz) entrained network oscillatory theta activity between IPS and the premotor cortex (PMC) and caused the enhancement of individual performance in the manipulation of auditory items in working memory (*6*) [see also (*3*–*7*) for converging evidence from other tasks].

Another—and so far unrelated—vein of research consists of entraining brain oscillations with rhythmic sensory presentations, instead of electrical or magnetic external stimulation, with the aim of detecting entrained sensory circuits via frequency tagging (*9*) and/or registering their behavioral consequences (*10*). To date, this approach has been used essentially to study visual (*11*–*14*), auditory (*15*–*19*), or multisensory (*20*) perceptual mechanisms, but not higher-order cognitive processes such as memory. Unlike TMS, approaches based on sensory stimulation are expected to drive, via natural communication signaling only, cortical nodes connected directly or secondarily to sensory pathways at various depths of the brain network hierarchy.

Here, we inquired whether sensory stimulation in one modality (vision) would entrain supramodal regions to cause behavioral changes in another modality (audition)—with supramodal meant to designate brain areas activated by a remarkable diversity of cognitive tasks [see, e.g., multiple-demand system (*21*) and superordinate frontotemporal network (*22*) (Fig. 1A)]. The IPS is one of such supramodal regions involved in a variety of manipulation tasks such as auditory working memory (*23*) and visual mental rotation (*24*, *25*). In the present study, we ran three experiments substituting rh-TMS with rhythmic (5-Hz, theta-range) flickering visual presentations of rotating three-dimensional (3D) shapes known to activate the IPS (*24*, *25*). We targeted theta oscillations in the dorsal pathway because increased frontoparietal theta power during the memory retention period is observed with increased memory load and working memory demands (*5*, *26*, *27*). In a related vein, frontoparietal theta phase locking during working memory tasks supports long-range connectivity between nodes of the central executive network (*28*, *29*). In the present study, our objective was to entrain theta oscillatory activity specifically in the dorsal stream, with visual stimulations (experiment 1) to cause behavioral enhancement of auditory working memory functions (experiments 2 and 3).

RESULTS

Rhythmic visual stimulation entrains the dorsal cortical pathway

In experiment 1, we studied the entrainment of oscillatory neurophysiological activity induced by 5-Hz flickering visual stimuli

[1]Cognitive Neuroscience Unit, Montreal Neurological Institute, McGill University, Montreal, QC H3A 2B4, Canada. [2]McConnell Brain Imaging Center, Montreal Neurological Institute, McGill University, Montreal, QC H3A 2B4, Canada. [3]International Laboratory for Brain, Music and Sound Research (BRAMS), CRBLM, Montreal, QC H2V 2J2, Canada. [4]CERVO Brain Research Centre, School of Psychology, Laval University, Québec, QC G1J 2G3, Canada.
*Corresponding author. Email: philippe.albouy@psy.ulaval.ca
†These authors contributed equally to this work.

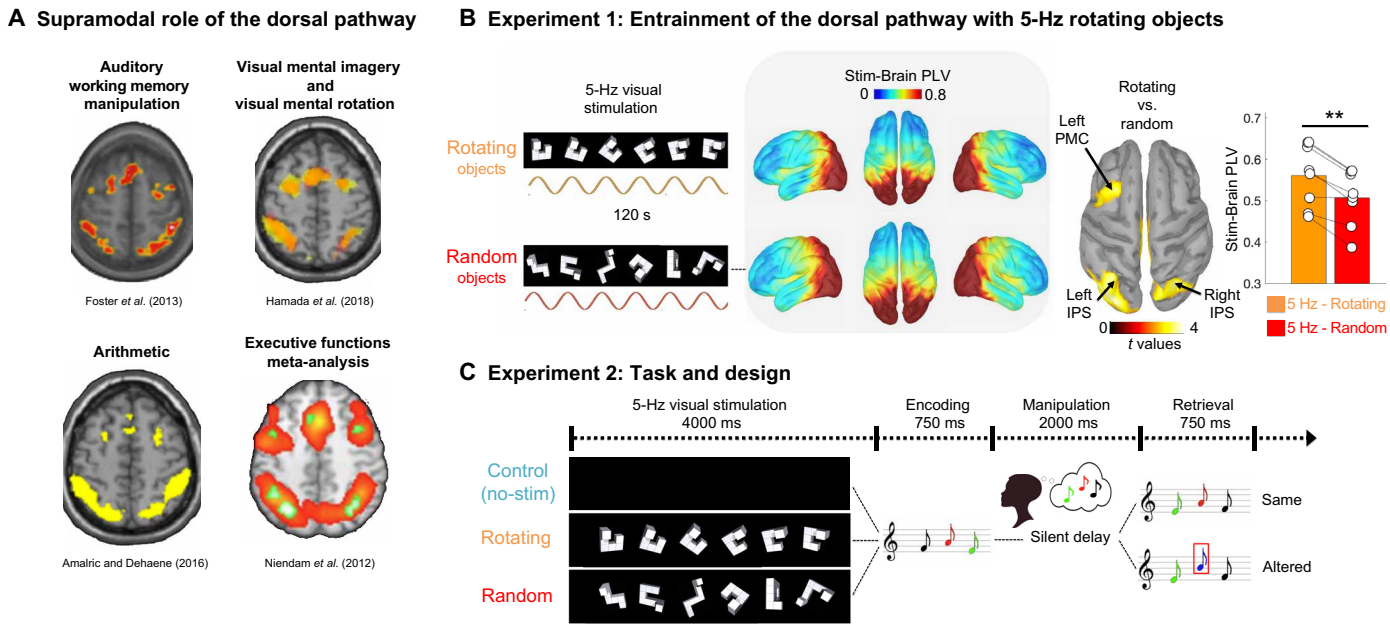

Fig. 1. Rhythmic visual stimulation entrains the dorsal cortical pathway. (**A**) Dorsal pathway brain regions are involved in a wide range of cognitive tasks, as illustrated from a selection of fMRI studies of auditory working memory (*23*), visual mental imagery and rotation (*24*), and arithmetic (*28*) and executive functioning (*22*) (see the Supplementary Materials for details). (**B**) Experiment 1: In each trial, participants passively observed either the same rotating Shepard's object (*26*) or a random selection of Shepard's objects (in both cases, 120-s stimulation duration and flickering at 5 Hz). Left: Stim-Brain PLV scores at 5 Hz were extracted for each of the MEG cortical sources. Right: Rotating versus random Stim-Brain PLV contrast revealed dorsal stream regions ($P < 0.05$ uncorrected for illustration). Bar plot shows Stim-Brain PLV (average of significant regions: left IPS, right IPS, and left PMC) for the rotating (orange) and random (red) conditions. White dots represent individual data; all participants showed the effect (eight of eight). (**C**) Experiment 2: Participants performed an auditory working memory task under three conditions: (i) without visual stimulation [control condition (no-stim), top panel], (ii) after presentation of 5-Hz rhythmic visual stimulation (rotating, middle panel), and (iii) after presentation of random shapes (random, bottom panel) over the first 4 s of each trial. They then listened to a three-note melody and had to mentally reverse the sequence over the next 2 s. In "same" trials, the second auditory sequence consisted of the same tones as in the first melody but in reversed temporal order; in "different" trials, the melody was also reversed, but the pitch of one of the tones was different from that in the original sequence.

distally from occipital visual areas along the dorsal pathway. Eight healthy individuals (see Materials and Methods) passively observed 3D geometric shapes [3D Shepard's objects (*30*)] flickering at 5 Hz on a video display during an MEG recording (Fig. 1B). In the rotating condition, the same object was perceived as rotating around its centroid during the entire stimulation time period (120 s, 20° rotation clockwise between two consecutive frames). In the random condition, different Shepard's objects were presented randomly in each frame (5 Hz), thus not giving rise to a sensation of rotation. We estimated the stimulation-to-brain phase-locking value (Stim-Brain PLV) to investigate the effects of these rhythmic visual stimulations on the phase of neurophysiological activity [Stim-Brain PLV extracted from MEG source time series; see Materials and Methods and (*6*) for a similar procedure].

In both the rotating and random conditions, we observed Stim-Brain PLV entrainment at 5 Hz across a broad set of posterior brain areas from occipital to dorsal stream regions (Fig. 1B) (*22*–*24*, *31*). Contrasting the rotating versus random conditions further revealed an increased expression of Stim-Brain PLV during the visual presentation of rotating objects, as predicted, specifically over bilateral IPS (left: $x = -26$, $y = -62$, $z = 44$; $t = 2.90$; $P = 0.01$; right: $x = 34$, $y = -62$, $z = 40$; $t = 3.48$; $P = 0.005$) and left PMC ($x = -42$, $y = -22$, $z = 28$; $t = 4.61$; $P = 0.001$) using their respective brain coordinates from (*22*) (see Materials and Methods). This contrast was not significant for right PMC ($x = 26$, $y = 42$, $z = 20$; $P = 0.11$).

Theta band activity across the dorsal cortical pathway predicts manipulation abilities in working memory

In experiment 2, we investigated whether (i) theta band activity in dorsal supramodal regions was related to auditory working memory task performance and (ii) the entrainment of this theta band activity with rhythmic sensory stimulation resulted in behavioral enhancements in a task involving a different sensory modality. Specifically, we asked whether the rhythmic visual stimulations used in experiment 1 could enhance manipulation abilities of auditory items in working memory. Twenty-three healthy individuals (Materials and Methods) performed an auditory working memory manipulation task under three different conditions (control, rotating, and random; Fig. 1C) with simultaneous EEG recording.

In the control condition (no stimulation), theta band (4 to 8 Hz) activity over frontoparietal electrodes and bilateral IPS sources during the silent manipulation period was positively correlated with behavioral task performance (significant time window between 1000 and 1500 ms; $P < 0.05$, cluster-corrected; 1000 permutations; alpha = 0.05; cluster size: sensors—left cluster, $k = 10$ electrodes; sensors—right cluster, $k = 2$ electrodes; sources—left IPS, $k = 813$ vertices, 129.49 cm^2; sources—right IPS, $k = 376$ vertices, 120.80 cm^2; Fig. 2A). During the same manipulation period, we derived interregional connectivity (PLV) from the EEG source maps between the average activity of bilateral IPS (as seed) and the rest of the brain (*6*, *32*). We found that theta band PLV connectivity between bilateral

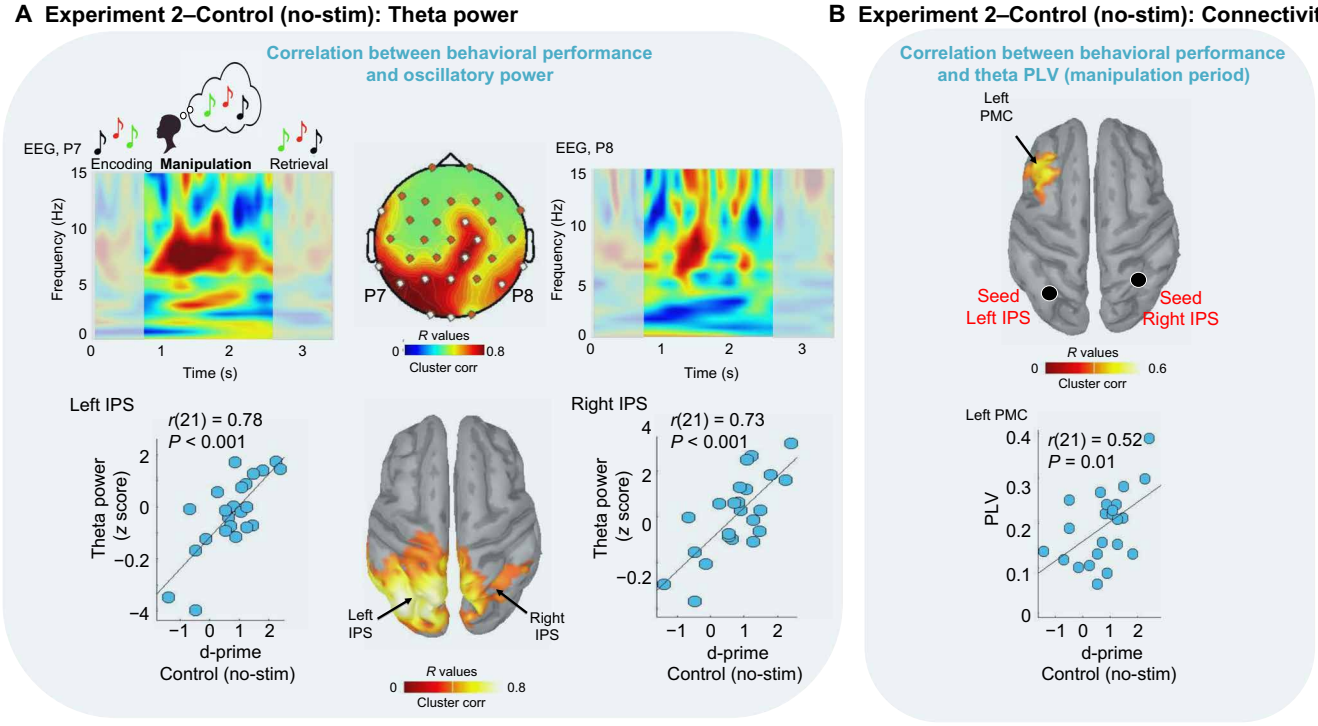

Fig. 2. Fronto-parietal theta band activity predicts working memory performance. (**A**) EEG data of the control (no-stim) condition. Top: EEG topography (center display, averaged over the significant 1000- to 1250-ms time window, cluster-corrected $P < 0.05$) and time-frequency representation (left and right displays, for a trial time window: 0 to 3500 ms) of correlation scores (*R* values) between the power of EEG signals shown at representative electrodes P7 and P8, and behavioral performance. Bottom: Whole-brain correlation between behavioral performance and theta band signal power (Hilbert transform in the theta band 4 to 8 Hz, averaged over the significant 1000- to 1250-ms time window) at the source level ($P < 0.05$, cluster-corrected). Scatter plots of performance in the control (no-stim) condition against theta power in the left and right IPS. (**B**) Whole-brain correlation ($P < 0.05$, cluster-corrected) between theta PLV with bilateral IPS during the manipulation period (750 to 2750 ms) and behavioral performance in the control (no-stim) condition. Scatter plot of performance in the control (no-stim) condition against theta PLV (seed bilateral IPS) in the left PMC.

IPS and left PMC was positively correlated with individual behavioral performances [$P < 0.05$, cluster-corrected, 1000 permutations, alpha = 0.05, cluster size, $k = 332$ vertices, 35.78 cm^2; $r(21) = 0.52$, $P = 0.01$ at cluster peak; Fig. 2B].

Rhythmic visual stimulation causally enhances auditory working memory performance

We then investigated the effects of visual stimulation on behavioral performance (using d-prime; Fig. 3A) with a repeated-measures analysis of variance (ANOVA) [with condition (control, rotating, random) as within-participant factor]. The main effect of condition was significant $F(2,44) = 4.66$, $P = 0.01$, $\eta 2 = 0.07$: Performance was increased in rotating versus control ($P = 0.03$, Tukey-corrected, with 17 of 23 participants showing the effect) and rotating versus random ($P = 0.02$, Tukey-corrected, with 16 of 23 participants showing the effect; Fig. 3A). Individual task accuracy in the control and random conditions was not statistically different ($P = 0.99$).

Causal relationship between oscillatory entrainment and behavioral benefits

During the visual stimulation time period (−4000 to 0 ms), we found that theta power over parietal EEG sensors and over the left IPS was predictive of individual task performance only for the rotating condition ($P < 0.05$, cluster-corrected; fig. S2B). There was no such effect either in the random condition or following visual stimulation in all conditions.

To evaluate entrainment per se, we then estimated Stim-Brain PLV for the entire post-visual stimulation time period (0 to 3500 ms, corresponding to the duration of a working memory trial). Stim-Brain PLV was estimated after the offset of 5-Hz rhythmic visual presentations using a 5-Hz sinusoid time series as an ongoing proxy reference signal in phase with preceding flickering visual presentations (Materials and Methods). We then produced whole-brain maps of correlation scores between Stim-Brain PLV and task performance.

In the rotating condition, whole-brain analysis revealed that Stim-Brain PLV in bilateral IPS and left PMC was positively correlated to behavioral performance [cluster-corrected $P < 0.05$, 1000 permutations, alpha = 0.05; cluster sizes: left IPS, $k = 238$ vertices, 36.65 cm^2; right IPS, $k = 382$ vertices, 60.04 cm^2; left frontal, $k = 330$ vertices, 52.08 cm^2; right frontal, $k = 186$ vertices, 32.96 cm^2; average of significant clusters: $r(21) = 0.63$; $P < 0.001$; Fig. 3B]. No significant whole-brain effect was observed in the random condition. To further compare the rotating and random conditions, we performed the correlation between behavioral performance and Stim-Brain PLV in the random condition from the cluster of regions revealed in the rotating condition (i.e., bilateral IPS and left PMC). This confirmed the absence of significant correlation between neural entrainment in the dorsal pathway and behavioral performance in the random condition [$r(21) = 0.11$, $P = 0.60$; Fig. 3B, right panel]. A Fisher *r*-to-*z* transformation performed on the *r* values of the rotation and random conditions further revealed that the difference between the two correlation coefficients was significant ($z = 2.02$, $P = 0.03$).

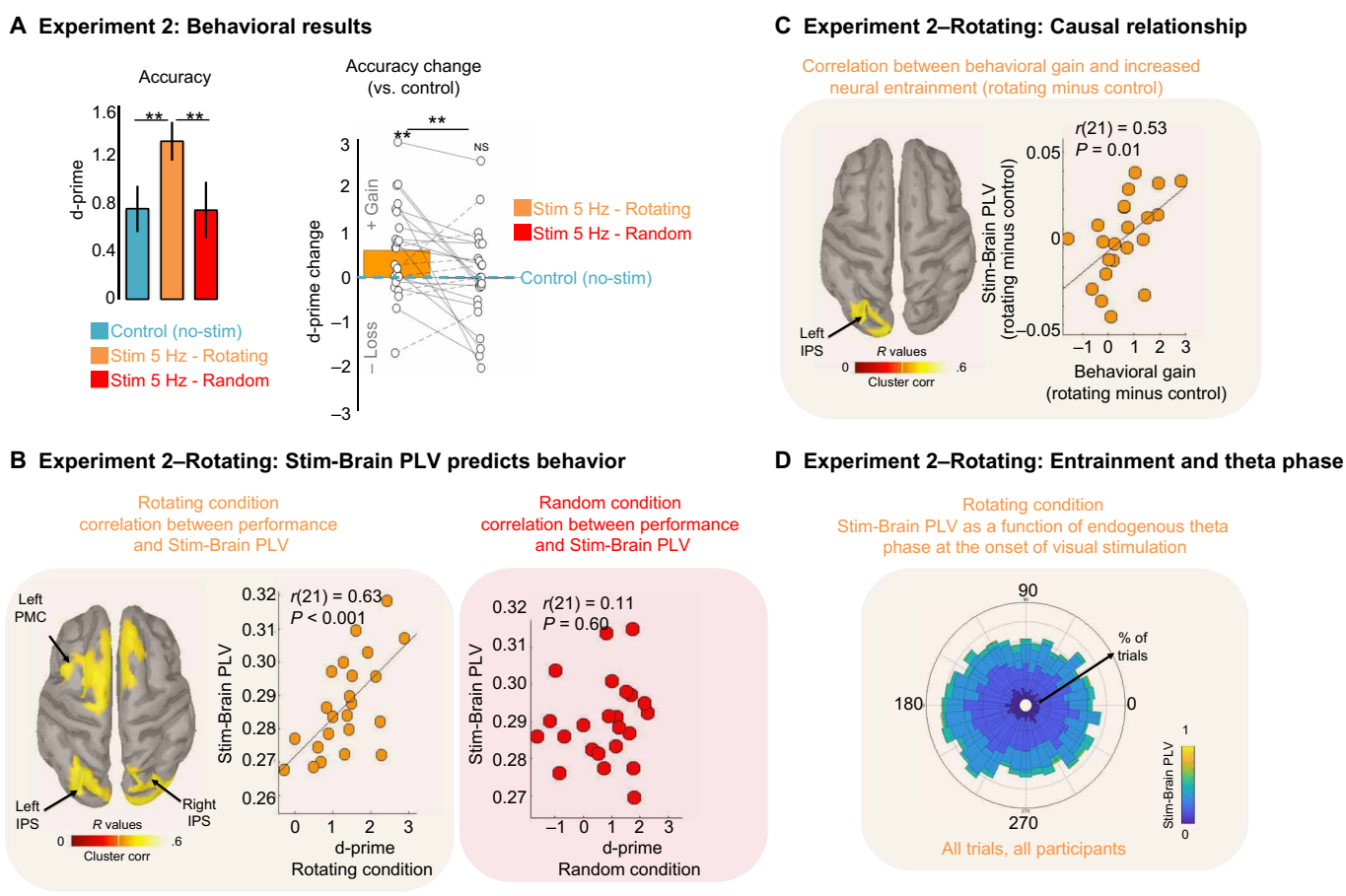

Fig. 3. Rhythmic visual stimulation causally enhances theta activity and working memory performance. (**A**) Left: Mean performance (d-prime) on the auditory working memory task for the control condition (blue), the rhythmic visual simulation with rotating objects (orange), and the rhythmic visual simulation with random objects (red). Error bars indicate SEM. Stars indicate significance (all $P < 0.02$). Right: Changes in task performance accuracy in the rotating and random visual presentation conditions relative to the control condition (positive values represent a gain in task performance; negative values represent a loss in task performance). Dots indicate individual data. Solid lines indicate participants who showed increased performance in the rotating versus random condition (15 of 23). Dashed lines indicate participants showing decreased performance for the same comparison (8 of 23). NS, not significant. (**B**) Left: Whole-brain correlation at the source level between behavioral performance and 5-Hz Stim-Brain PLV for the rotating condition ($P < 0.05$, cluster-corrected). Middle: Scatter plot of performance for the rotating condition against Stim-Brain theta PLV (average of bilateral IPS and left PMC). Right: Scatter plot of performance (average of bilateral IPS and left PMC identified in the rotating condition) for the random condition against Stim-Brain theta PLV. (**C**) Whole-brain correlation ($P < 0.05$, cluster-corrected) and scatter plots of behavioral benefits (versus control) against Stim-Brain PLV entrainment (versus control) for the rotating condition. (**D**) Stim-Brain PLV as a function of theta phase at visual stimulation onset. The circular histogram, across participants and trials, represents the theta phases measured in bilateral IPS and left PMC. Color map represents the strength of Stim-Brain PLV.

Last, in the rotating condition, a whole-brain analysis revealed that the entrainment gain (with respect to the control condition) was positively correlated with individual differences in behavioral enhancement (versus control) in the left IPS [cluster-corrected, 1000 permutations, alpha = 0.05; cluster size, $k = 165$ vertices, 26.39 cm^2, $P < 0.05$; $r(21) = 0.53$, $P = 0.01$; see Fig. 3C].

We then asked whether stronger entrainment of the dorsal stream would be contingent on the phase of theta cycles at the onset of rhythmic visual presentations (see Materials and Methods). We observed that the entrainment of the dorsal stream (Stim-Brain PLV in bilateral IPS and left PMC) was independent of the phase of theta cycles at the onset of rhythmic visual presentations [repeated-measures ANOVA, $F(7,154) = 0.45$, $P = 0.86$; Fig. 3D and Materials and Methods]. This observation is compatible with models of neural entrainment subsequent to the resetting of the phase of oscillations by the onset of an external stimulus (*33*).

Rhythmicity, frequency of the stimulation, and rotating properties of the visual stimulation support the stimulation-related behavioral gain

In experiment 3, we investigated whether the rhythmicity and the frequency of the visual presentation (theta), and not only the rotating properties of the stimulus, support the behavioral enhancement observed in experiment 2. We ran a separate behavioral study with an independent sample of participants and asked whether the enhancement of manipulation abilities of auditory items in working memory [as compared to the control (no-stim) condition] was specific to the presentation of rotating visual objects at 5 Hz (experiment 2, 5Hz-rotating condition). To that end, we designed two additional experimental conditions with the same rotating visual objects presented either at a 1-Hz rate (1Hz-rotating condition) or as continuously rotating (i.e., with no flicker; continuous-rotating condition). Twelve healthy individuals (Materials and Methods) performed the

same auditory working memory manipulation task as in experiment 2 under four different conditions: no-stim, 5Hz-rotating, continuous-rotating, and 1Hz-rotating (Fig. 4A).

We investigated the effects of visual stimulation on behavioral performance (Fig. 4B) with a repeated-measures ANOVA with condition (no-stim, 5Hz-rotating, 1Hz-rotating, and continuous-rotating) as within-participant factor. The main effect of condition was significant, $F(3,36) = 3.75$, $P = 0.01$, $\eta 2 = 0.01$: Performance was increased in the 5Hz-rotating versus control (no-stim) condition ($P = 0.02$, Tukey-corrected) and the 5Hz-rotating versus 1-Hz rotating ($P = 0.003$) condition and was not significant between the 5Hz-rotating and continuous-rotating ($P = 0.10$) condition. Individual task accuracies in the control (no-stim), 1Hz-rotating, and continuous-rotating conditions were not statistically different (all with $P > 0.30$). We further report the behavioral gains induced by the rhythmicity and the frequency of the rotating stimulation with observed changes in task performance accuracy in all three rotating conditions with respect to the control (no-stim) condition (Fig. 4B, right panel). A repeated-measures ANOVA with condition [5Hz-rotating minus control (no-stim), continuous-rotating minus control (no-stim), and 1Hz-rotating minus control (no-stim)] as within-participant factor revealed a significant main effect of condition, $F(2,22) = 9.66$, $P < 0.001$, and $\eta 2 = 0.105$. Performances were significantly greater in the 5Hz-rotating versus continuous-rotating condition ($P = 0.008$, Tukey-corrected, with 11 of 12 participants showing the effect) and the 5Hz-rotating versus 1Hz-rotating condition ($P < 0.001$, Tukey-corrected, with 11 of 12 participants showing the effect; Fig. 4B).

DISCUSSION

The present study investigated (i) whether supramodal brain structures along the dorsal pathway, which mediate a remarkable diversity of cognitive tasks [such as the multiple-demand system (*21*)], can

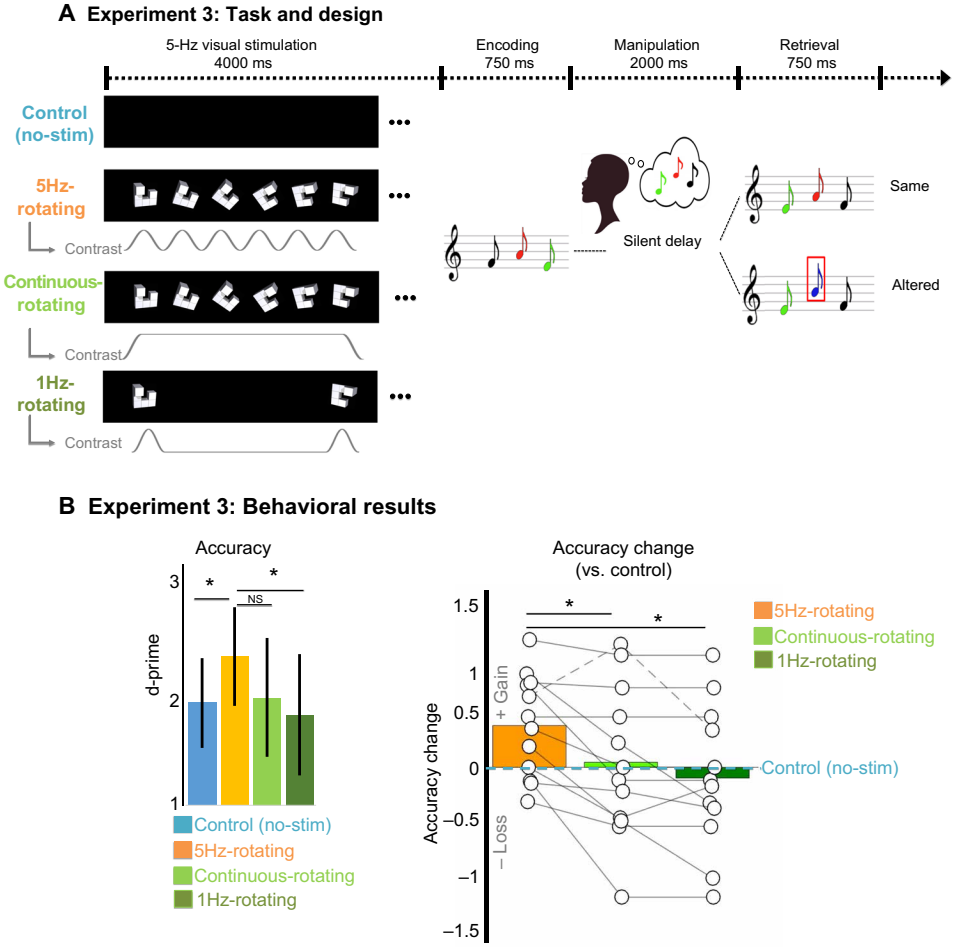

Fig. 4. Stimulation rhythmicity and frequency support the behavioral gains. (**A**) Experiment 3: Participants performed the auditory working memory task described in experiment 2 under four conditions: (i) without visual stimulation [control condition (no-stim), in blue], (ii) after presentation of a 5-Hz rhythmic rotating visual stimulation as in experiment 2 (5Hz-rotating, in orange), (iii) after presentation of a continuously rotating visual stimulation (continuous-rotating, in light green), and (iv) after presentation of a 1-Hz rhythmic rotating visual stimulation (1Hz-rotating, in dark green) over the first 4 s of each trial. (**B**) Performance (d-prime) on the auditory working memory task for the control condition (blue), the 5-Hz rhythmic visual simulation with rotating objects (orange), the continuous-rotating visual simulation (light green), and the 1-Hz rhythmic visual simulation with rotating objects (dark green). Error bars indicate SEM. Stars indicate significance (all $P < 0.05$). Right: Changes in task performance accuracy in the 5Hz-rotating, continuous-rotating, and 1Hz-rotating visual presentation conditions relative to the control condition (positive values represent a gain in task performance; negative values represent a loss in task performance). Dots indicate individual data. Solid lines indicate participants who showed increased performance (relative to control) in the rotating versus continuous and versus 1-Hz condition (11 of 12). Dashed lines indicate participants showing decreased performance for the same comparison (1 of 12).

be selectively and rhythmically entrained by sensory stimulation in a given modality (here, vision, experiment 1), (ii) whether this entrainment can causally enhance behavioral performance in a working memory task involving another sensory modality (here, audition, experiment 2), and (iii) whether the effect is driven by both the rotating properties of the visual stimulus and its frequency of presentation (flickering at 5 Hz, experiment 3).

We first demonstrate with MEG (experiment 1) that the flickering visual presentation of rotating 3D shapes entrained brain oscillations and enhanced network connectivity in supramodal brain regions at the stimulation frequency, distally from the occipital cortex. This result is in line with the concept of supramodality of neural entrainment (*2*), proposing that rhythmic sensory stimulation can reach supramodal brain regions and modulate brain activity beyond sensory areas. While it has been suggested that the timing of inputs in one sensory modality can guide the processing of concurrent or subsequent inputs in other modalities, the present results show that the entrainment can reach and modulate activity in dorsal stream structures. In experiment 2, we thus tested whether this modulation of the frontoparietal activity with visual rhythmic stimulation can positively affect the processing of auditory items in memory.

We first show that theta band activity (magnitude and PLV) in dorsal supramodal regions was related to auditory working memory task performance. These data confirm and replicate previous findings showing that regional theta power (IPS) and frontoparietal connectivity in the theta range (between bilateral IPS and PMC) predict individual manipulation abilities during working memory [see (*5*, *6*, *23*, *31*, *34*–*36*)]. So far, however, these associations remain correlative. To investigate whether rhythmic visual stimulation can causally modulate oscillatory activity in these pathways [as previously shown in rh-TMS and transcranial alternating current stimulation studies (*3*–*7*)] and in consequence modulate behavior, we investigated the effect of theta rhythmic visual stimulation (as in experiment 1) applied before each trial of the working memory task.

We show that rotating visual stimulation increased behavioral performance as compared to the control condition and to the random stimulation condition. These results constitute strong behavioral evidence of working memory improvement induced by rhythmic visual stimulation (Fig. 3A). The present data are aligned with prior studies of associations between oscillatory entrainment outcomes and enhancement of behavioral performance (*3*, *4*, *7*, *8*). Their specific novelty is in suggesting that rhythmic visual stimulation can modulate theta activity in a brain network recruited during the manipulation of auditory stimuli, and thus suggests that the two cognitive processes (visual rotation and auditory working memory) share a common supramodal neural network. We therefore tested this latter hypothesis in the EEG data by investigating the potential neurophysiological mechanism underlying the observed behavioral effect.

By combining EEG and behavioral measures, we show that rhythmic visual presentation of rotating shapes immediately before each trial of an auditory working memory task entrains theta activity across the same dorsal brain pathway and causally enhances task performance. We found that the strength of stimulation-induced neurophysiological entrainment scales with behavioral enhancement in the auditory working memory task. These effects were not observed when presenting random, nonrotating, 3D shapes at the same rhythmic rate. These results suggest that rhythmic visual stimulation in the theta range promotes oscillations in the dorsal cortical pathway and enhances performance in an auditory working memory manipulation task. This effect is specific to the presentation of rotating visual shapes, because they engage a cognitive mechanism that is relevant to that neural circuit (*24*). Specifically, the causal relationship between theta PLV and behavior was observed in the left IPS. This finding is similar to our previous study using TMS where the stimulation over the left IPS during task performance (with the same behavioral task) (*6*) causally boosted participants' behavioral performance. This is in line with the central role of IPS in working memory manipulation: For working memory, while the posterior parietal cortex (including the IPS) has been originally identified as a short-term memory store (*37*) supporting memory maintenance (*38*–*41*), recent studies have highlighted its specific contribution to memory manipulation processes (*6*, *23*, *31*, *42*, *43*).

Overall, experiment 2 shows that theta rhythmic visual stimulation with rotating objects presented before each trial of an auditory memory task entrains distributed theta range activity across the dorsal cortical pathway and causally enhances auditory manipulation abilities in memory. In addition to providing further evidence of a causal relationship between brain oscillatory activity and behavior (*3*), our data emphasize the supramodal functions of the human dorsal pathway.

These findings are in line with other recent functional neuroimaging studies of the human dorsal stream being engaged across a variety of cognitive tasks (Fig. 1A) (*21*, *44*). Niendam and colleagues identified a "superordinate frontoparietal network" from overlapping activity patterns extracted from 193 functional magnetic resonance imaging (fMRI) studies (*22*). This network, also labeled as the "multiple-demand system" (*21*), is proposed to support a wide range of different tasks that involve common cognitive processes—a concept that accounts, in part, for the distributed nature of brain activity related to cognitive control functions (*45*). Our present data further support this notion by showing not only that the same brain pathway is involved in distinct tasks but also that activation by one of these tasks can transfer to the enhancement of performance in another task.

However, a possible counterargument could be that any visual presentation of a 3D rotating object would be sufficient to preactivate the dorsal network and therefore induce performance enhancement in the auditory working memory task. From the three experimental conditions used in experiment 2 (control, random, and rotating), only the rotating condition included a stimulus known to activate the dorsal stream (3D rotating visual stimulus) and specifically the IPS. In experiment 3, we investigated this question by comparing behavioral performance in the no-stim condition to those observed in the 5Hz-rotating, 1Hz-rotating, and continuous-rotating conditions. First, we replicated the behavioral results of experiment 2 in an independent sample of subjects: Participants showed higher performance in the 5Hz-rotating condition than in the no-stim condition. Second, there was no such effect in the continuous-rotating and 1Hz-rotating condition. Crucially, behavioral gains with respect to the no-stim condition were larger in the 5Hz-rotating condition than in either the continuous-rotating or 1Hz-rotating conditions. Together, these results confirm that both the rhythmicity of the 3D visual stimulation and its frequency (in the neurophysiological theta range) are crucial to the behavioral gains in auditory working memory.

Overall, our data reveal an association between frequency-specificity, different cognitive demands, and the supramodal nature of the dorsal pathway. A variety of hypotheses may be considered to

explain the observed effects. First, theta signaling may be the main communication channel between frontoparietal regions, regardless of the cognitive task. This would suggest that the effects reported here would generalize to other tasks and contexts. This would be in line with the supposed functional role of theta oscillations in the human brain as supporting long-range corticocortical communication (*28*, *29*). Second, the observed supramodal effect could be seen as driven by increased selective attention induced by visual stimulation. However, previous studies have shown that modulation of theta activity in the dorsal pathway induces task-specific neural entrainment and behavioral gain. Notably, using the same task but a different stimulation approach (rhythmic TMS over the left IPS) (*6*), we showed that rhythmic stimulation outcomes (in terms of entrainment and behavior) were specific to a task requiring mental manipulation (but not in a simple same/different control task that does not recruit the dorsal pathway). Therefore, enhancement induced by selective attention would be expected to be involved in both tasks, not only one. Because we observed comparable behavioral benefits and neural entrainment effects in two separate studies using the same task [here and in (*6*)], we make the hypothesis that the observed effects are not driven by attentional or other unspecific factors.

In the present study, we provide evidence that targeted rhythmic entrainment of a supramodal brain network in one sensory modality can be beneficial to the performance of a cognitive task in another modality. Whether such benefits can be long lasting remains to be studied. Future research will also show whether this approach can be extended and generalized to interventions on other brain systems and sensory modalities and whether this procedure can inspire a practical approach to transfer of learning in general, with potential for translational and clinical impact.

MATERIALS AND METHODS

Participants

Forty-three neurologically healthy young adults (nonmusicians, 41 right-handed, 24 women; mean age, 25.30 ± 4.32 years, ranging from 19 to 36 years old; mean education, 19.55 ± 3.47 years) participated in the study. Eight individuals participated in experiment 1, 23 individuals participated in experiment 2, and 12 individuals participated in experiment 3. All participants reported normal hearing, normal vision, and no history of neurological or psychiatric disease. They gave written informed consent and received a monetary compensation for their participation. All participants took part in a preliminary session to check for potential MEG artifacts (experiment 1) or to ensure that they were able to perform the auditory working memory task above chance level (experiments 2 and 3). Ethical approval was obtained from the Ethics Review Board of the Montreal Neurological Institute (NEU-14-043).

Methods details

Most EEG and MEG preprocessing, EEG/MEG source imaging, and statistical analyses were performed with Brainstorm (http://neuroimage.usc.edu/brainstorm/) (*46*) combined with FieldTrip functions (www.fieldtriptoolbox.org) and in-house MATLAB code.

Experiment 1: Protocol

During an MEG recording, the participants were asked to passively observe 3D shapes [Shepard's objects (*30*)] flickering on the screen at 5 Hz (Fig. 1B, white shapes with a 60 cd/m^2 luminance). In the first condition (rotating condition), the same object was rotating during the entire stimulation time period (120 s, 20° clockwise rotation between each frame). In the random condition, random Shepard objects were presented (a different object for each apparition on the screen). The Shepard's objects projected on a screen (1024 × 768 pixels located 75 cm in front of the participant) for 100 ms with a 200-ms inter-onset interval. The screen background color was black. Five minutes of resting-state data with eyes open was recorded at the beginning of each session (not used in present study). Presentation software (Neurobehavioral Systems, Albany, CA, USA) was used for delivery of the visual stimulation.

MEG recording (experiment 1)

Following procedures previously described in (*6*), participants were first tested for possible magnetic artifacts in a short preliminary MEG run. The MEG recordings were carried out using a 275-channel whole-head MEG system (CTF/VMS, Port Coquitlam, BC, Canada) with a sampling rate of 1200 Hz, a 0- to150-Hz filter bandwidth, and third-order spatial gradient noise cancellation. Concurrent horizontal and vertical electrooculograms (EOG) and electrocardiogram (ECG) were acquired with bipolar montages. Head position was determined with coils fixated at the nasion and the preauricular points (fiducial points). The positions of the fiducial coils were measured relative to the participant's head using a 3D digitizer (Polhemus Isotrack). About 150 additional scalp points were also digitized. Head position was monitored continuously (sampling rate: 150 Hz) and verified for consistency between blocks to ensure that head movements did not exceed 0.5 cm (this was confirmed by additional offline verification before further data analyses). Participants were seated upright in a sound-attenuated, magnetically shielded recording room and passively observed the visual stimuli projected on a screen. They were asked to keep their eyes open. The duration of experiment 1 was 15 min.

MEG preprocessing (experiment 1)

MEG data were preprocessed following good-practice guidelines (*47*) and using similar procedures as in (*6*) to verify data quality and to reduce contamination from artifacts (cardiac, eye movements and blinks, environmental noise). All recordings were visually inspected to detect segments contaminated by head movements or remaining environmental noise sources, which were discarded from subsequent analysis. Powerline contamination of the raw data (main, 60 Hz; harmonics at 120, 180, and 240 Hz) was reduced using notch filtering. Heart and eye movement (blink) contaminations were attenuated using signal-space projections from selected segments of data about each artifactual event (*46*). Heartbeat and eye blink events were automatically detected from the ECG and EOG traces, respectively. Projectors were defined using principal components analysis of these data segments filtered between 10 and 40 Hz (for heartbeats) or 1.5 and 15 Hz (for eye blinks) in a 160-ms time window centered about the heartbeat event or 400 ms around eye blink events (Brainstorm default parameters settings). The principal components that best captured the artifact's sensor topography were manually selected as the dimension against which the data were orthogonally projected away from. In all participants, the first principal component was sufficient to remove artifact contamination. The projectors obtained for each participant were propagated to the corresponding MEG source imaging operator. The preprocessed data were then band pass–filtered between 0.3 and 50 Hz with a second-order Butterworth filter (12 dB/octave slope) and down-sampled to 500 Hz.

MEG source imaging (experiment 1)

Source reconstruction was performed using functions available in Brainstorm, all with default parameter settings (*46*), as in (*6*). Forward modeling of neural magnetic fields was performed using the overlapping-sphere technique. The lead fields were computed from elementary current dipoles distributed perpendicularly to the cortical surface from each individual. MEG source imaging was performed by linearly applying Brainstorm's weighted minimum norm operator onto the preprocessed data. The data were previously projected away from the spatial components of artifact contaminants. For consistency between the projected data and the model of their generation by cortical sources, the forward operator was itself projected away from the same contaminants using the same projector as for the MEG data. The MEG data were projected on a cortical surface template available in Brainstorm (adult cortical surface of 15,002 vertices serving as image support for MEG source imaging).

Stim-Brain PLV (experiment 1)

Source reconstruction was applied to preprocessed MEG data (one trial of 120 s for each condition). To estimate the effects of visual stimulation on the phase of MEG signals, we estimated the PLV between a pure sinusoidal signal at 5 Hz (simulating the visual stimulation) and brain activity. Stim-Brain PLV whole-brain maps from the rotating and random conditions were contrasted using vertex-wise *t* statistics (t/p maps) for illustration, and significance was estimated with a region-of-interest (ROI) approach using coordinates from Niendam *et al.* (*22*): left IPS ($x = -26$, $y = -62$, $z = 44$), right IPS ($x = 34$, $y = -62$, $z = 40$), left PMC ($x = -42$, $y = -22$, $z = 28$), and right PMC ($x = 26$, $y = 42$, $z = 20$). The regional average of the Stim-Brain PLV across all 50 vertices of each ROI was extracted and used for deriving a contrast measure between the rotating and random conditions for each region.

Experiment 2: Protocol

Participants performed an auditory working memory task [from (*6*)] under three different conditions during an EEG recording. The task required the manipulation of auditory information in which the listener must identify a local pitch change in two patterns that always differ in temporal order (see below). In the control condition, participants performed the auditory task without visual stimulation. During the rotating and random stimulation conditions, participants performed the same auditory task under theta visual stimulation with rotating Shepard's objects or with random Shepard's objects (as in experiment 1), respectively. The visual stimulation was delivered for 4 s before the onset of the first auditory sequence (Fig. 1C). There were three main goals to this recording session: (i) evaluate task performance and collect EEG data without applying stimulation, (ii) confirm the frequency of the neural oscillatory signal markers related to the auditory task, and (iii) evaluate the effects of the visual stimulation on behavior and neural oscillatory activity. EEG data without visual stimulation were used as control condition and were compared across sensor and source levels to the two conditions with visual stimulation.

Auditory stimuli (experiment 2)

Stimuli were taken from (*6*). All melodies were composed of three 250-ms piano tones presented successively without inter-tone interval. Sixty different melodies (sequences) were created using piano timbre and differed in pitch height (Sibelius, http://www.sibelius.com, tones from C4 to E6). These 60 sequences were used as the first melody of the pair (S1) and were the same for the different stimulation condition (control, rotating, random). All sequences were structured (tonal) according to the Western musical system; the pitch interval between consecutive tones was always inferior to 12 semitones (an octave), and identical tones were not repeated consecutively in a sequence.

Manipulation task experiment 2

The task consisted of a same-different auditory melodic discrimination task [see (*6*); example stimuli of the manipulation task in Fig. 1C]. Participants were asked to detect whether the pitch of one of the tones had been changed in the second melody (S2; pitch change of two or three semitones). The change, when applied, preserved the melodic contour (the order of upward and downward pitch movement in a melody without regard to magnitude). The tones of the second melody were always reversed in time so that the final tone became the first. This transformation required a comparison between a sample and a transformed target. Therefore, participants had to manipulate auditory information in memory during the task. The changed tone in the reversed melodies could be that at any of the three possible positions.

Procedure for experiment 2

Procedures in experiment 2 were similar to those reported in (*6*). Presentation software (Neurobehavioral Systems, Albany, CA, USA) was used to deliver visual and auditory stimuli and triggers and register button presses. For each trial, participants listened binaurally to the first three-tone sequence over a duration of 750 ms (encoding, S1), followed by a silent retention period of 2000 ms and the second melodic sequence (retrieval, S2, 750-ms duration). As mentioned above, in the control condition, participants performed the auditory task without visual stimulation. During the rotating and random conditions, participants performed the same auditory task following 5-Hz visual stimulation with rotating or random Shepard's objects (as in experiment 1), respectively. Visual stimulation lasted 4 s before the onset of the first auditory sequence (Fig. 1C). We collected one block of 60 trials of each of the conditions (control, rotation, random). The blocks were separated by ~3-min breaks. The different conditions were presented in alternation (counterbalanced across participants). Participants were informed of condition order and asked to indicate their answers by pressing one of two keys with their right hand after the end of S2. They had 2 s to respond before next trial onset, which occurred 2.5 to 3 s after the end of S2. No feedback was given during the experiment. In each block, 60 trials were presented (30 identical melodies and 30 altered melodic pairs). Within each block, the trials were presented in a pseudo-randomized order, with the same trial type (i.e., same and different) not repeated more than three times in a row. Before the session, participants performed a set of 15 practice trials (using melodies not presented subsequently in the main experiment) without feedback. Behavioral data were analyzed with d-prime (signal detection theory) and repeated-measures ANOVA.

Visual stimulation experiment 2

Rhythmic visual stimulations were delivered over 4 s before each trial of the auditory working memory task. The duration of visual stimulation was defined with pilot testing (see fig. S1). Participants were seated with their chin positioned in a chin rest, their eyes open, and their gaze centered on a continuously displayed fixation cross (gray on a black background). They listened to the auditory stimuli presented binaurally through air-conducting tubes with foam ear tips [70-dB sound pressure level, as in (*6*)]. They were asked to maintain central fixation and to minimize eye blinks and other body

movements during the recording blocks. In the control condition, no visual stimulation was delivered during the 4 s preceding each trial of the auditory working memory task (black screen). In the rotating and random conditions, each trial of the working memory task was preceded by 4 s of rhythmic visual stimulation. For each trial, 20 image frames were delivered with 100-ms duration, 200-ms inter-onset interval, resulting in 5-Hz flickering visual stimuli (Fig. 1C). The 36×27 cm^2 cathode ray tube computer screen (1024×768 pixels) was located 65 cm in front of the participant. The screen background color was black. The visual stimuli were the same white Shepard objects of 60 cd/m^2 luminance as in experiment 1.

EEG recordings experiment 2

We used active electrodes with BrainAmp 32 DC amplifiers (Brain Products, www.brainproducts.com). EEG was continuously acquired from 32 channels (in addition to ground, EOG, and nose reference electrodes). The signal was band pass–filtered between DC and 1000 Hz and digitized at a sampling rate of 1000 Hz. Skin/electrode impedance was maintained below 5 kilohms. The positions of the EEG electrodes were registered using the same 3D digitizer system (Polhemus Isotrack) [see (*6*)].

EEG preprocessing

Following procedures previously described in (*6*), preprocessing included reduction of powerline contamination of the raw data (main, 60 Hz; harmonics at 120, 180, and 240 Hz) using notch filtering. Data were subsequently filtered between 0.3 and 80 Hz and subjected to independent components analysis using EEGLAB (https://sccn.ucsd.edu/eeglab) for the removal of artifacts (eye movements/blinks). Using time-course and topographic information, components representing clear ocular artifacts were identified and removed from the filtered data. Residual artifactual trials were removed by visual inspection. Individual EEG trials were then automatically inspected from −5000 to 4000 ms with respect to the onset of the first S1 tone. Trials with EEG values exceeding ±200 μV were excluded: Between 47 and 60 trials were kept for each participant and condition.

EEG oscillatory activity (experiment 2)

We were first interested in confirming the role of theta oscillations during the manipulation of information in memory. We thus focused on theta activity during the silent period between the presentation of the two melodies within a trial [see (*6*)]. We performed wavelet time-frequency decompositions of sensor signals (*48*). The EEG signals were convoluted with complex Morlet's wavelets, with a Gaussian shape in both the time (SD σt) and frequency domains (SD σf) around its central frequency $f0$. The wavelet family was defined by $(f0/\sigma f) = 7$, with $f0$ ranging between 2 and 80 Hz in 1-Hz steps. The time-frequency wavelet transform was applied to each trial and then averaged across trials, resulting in an estimate of oscillatory magnitude at each time sample and at each frequency bin between 2 and 80 Hz. Time-frequency decompositions of signal during the retention period were *z*-scored with respect to a prestimulus baseline (−5000 to −4000 ms before the presentation of the first tone). For the control condition, the resulting time-frequency maps were correlated to the individual behavioral performances (correlation applied at each frequency band and time sample), as illustrated in Fig. 2A. EEG signals were filtered in the theta frequency band (4 to 8 Hz) before their envelope was extracted using the Hilbert transform. The resulting signal magnitude envelopes were baseline-corrected using *z* scores with respect to the mean theta power over −5000 to −4000 ms preceding the presentation of the first tone. We derived a moving average version of these data over eight consecutive 250-ms time windows (between 750 and 2750 ms) during the manipulation period [see (*2*) for similar procedure]. For each time window, the resulting maps were correlated with individual behavioral performances in the control condition. Statistical significance was tested for each time window using cluster-level statistics (custom MATLAB code) on EEG topographies to account for multiple comparisons. We then performed the same analyses (Hilbert, correlation, cluster permutation testing) at the source level. The source reconstruction procedure and parameters were similar to those described in experiment 1, except that we used a realistic head model: symmetric boundary element method from the open-source software OpenMEEG. A realistic BEM model of head tissues and geometry for the MNI template was used, as EEG data are more sensitive to variations in head shape and tissue conductivity than MEG.

Functional connectivity

Functional connectivity during the retention period between bilateral IPS and the rest of the brain was investigated by estimating phase-locking statistics in the theta range (4 to 8 Hz, PLV) (*32*). PLV measures a degree of consistency (locking) in the difference in phase between time series (phase locking). This is realized by testing the significance of the covariance in phase between two signals, with a reasonable time resolution (~100 ms). PLV disentangles between phase and amplitude effects in interregional dependencies. PLV values were individually averaged across trials for each task and were then correlated with behavioral performances in the manipulation task. Stim-Brain PLV was extracted as in experiment 1 to estimate the effects of the visual stimulation on the phase of EEG signals at the sensor and source levels. We estimated PLV between a pure sinusoidal signal at 5 Hz (simulating rhythmic visual stimulation) and brain activity. To evaluate entrainment per se, Stim-Brain PLV was estimated for the entire post-visual stimulation time window (0 to 3500 ms, corresponding to the duration of a working memory trial). These data were then correlated with behavioral performance using cluster-level statistics.

Stim-Brain PLV as a function of the phase of theta oscillations

For the rotating condition in experiment 2, we investigated whether neural entrainment, as measured with Stim-Brain PLV, varied as a function of the phase of theta oscillations in bilateral IPS and left PMC at the onset of visual stimulation (see Fig. 3D and Results). This analysis allowed to investigate whether a preferred phase (in the clusters showing neural entrainment) at visual stimulation onset can be identified to elicit optimal entrainment of the dorsal stream or whether, as with rh-TMS, the stimulation induces a phase resetting of oscillations. For each trial, and each participant in the rotating condition, we extracted the phase of the theta at the onset of the visual stimulation and the Stim-Brain PLV (0- to 3500-ms time window). Circular statistics were then performed on the data of all participants to identify whether a preferred mean angle can be identified over the different trials. Then, we tested whether the amount of Stim-Brain PLV in the frontoparietal network varies as a function of theta phase at visual stimulation onset (theta phase sampled in eight bins).

Experiment 3

We investigated whether the rhythmicity and the frequency of the visual presentation (theta), and not only the rotating properties of the stimulus, support the behavioral enhancement observed in experiment 2 (see Results). We ran a separate behavioral study with an

independent sample of participants ($n = 12$) and asked whether the enhancement of manipulation abilities of auditory items in working memory [as compared to the control (no-stim) condition] was specific to the presentation of rotating visual objects at 5 Hz (experiment 2; 5Hz-rotating condition). To that end, we designed two additional experimental conditions with the same rotating visual objects presented either at a 1-Hz rate (1Hz-rotating condition) or as continuously rotating (i.e., with no flicker; continuous-rotating condition). The stimulus delivery, procedure, number of trials, and behavioral analyses were strictly identical to those reported in experiment 2.

Quantification and statistical analysis

The study includes $n = 43$ participants. Following procedures previously described in (*6*), behavioral statistical analyses were performed with repeated-measures ANOVA and using post hoc tests (Tukey-corrected). Correlations between functional data and behavioral data were estimated with Pearson's correlations. Statistical significance was set to $P \leq 0.05$. Analyses including behavioral data were computed using Jamovi and MATLAB.

Whole-brain analyses (sensors and sources) of oscillatory activity were performed with Pearson's correlation using cluster randomization statistics (1000 permutations, alpha = 0.05) as implemented in FieldTrip (www.fieldtriptoolbox.org). Statistical significance was set to $P \leq 0.05$ corrected for multiple comparisons. For all analyses (behavioral and functional), statistical values, dispersion, and precision measures (e.g., mean and SEM) can be found in the figures, figure legends, or main text.

SUPPLEMENTARY MATERIALS

Supplementary material for this article is available at https://science.org/doi/10.1126/sciadv.abj9782

View/request a protocol for this paper from *Bio-protocol*.

REFERENCES AND NOTES

1. V. Romei, G. Thut, J. Silvanto, Information-based approaches of noninvasive transcranial brain stimulation. *Trends Neurosci.* **39**, 782–795 (2016).
2. P. Lakatos, J. Gross, G. Thut, A new unifying account of the roles of neuronal entrainment. *Curr. Biol.* **29**, R890–R905 (2019).
3. S. Hanslmayr, N. Axmacher, C. S. Inman, Modulating human memory via entrainment of brain oscillations. *Trends Neurosci.* **42**, 485–499 (2019).
4. R. Polania, M. A. Nitsche, C. C. Ruff, Studying and modifying brain function with non-invasive brain stimulation. *Nat. Neurosci.* **21**, 174–187 (2018).
5. P. Albouy, S. Baillet, R. J. Zatorre, Driving working memory with frequency-tuned noninvasive brain stimulation. *Ann. N. Y. Acad. Sci.* **1423**, 126–137 (2018).
6. P. Albouy, A. Weiss, S. Baillet, R. J. Zatorre, Selective entrainment of theta oscillations in the dorsal stream causally enhances auditory working memory performance. *Neuron* **94**, 193–206.e5 (2017).
7. I. R. Violante, L. M. Li, D. W. Carmichael, R. Lorenz, R. Leech, A. Hampshire, J. C. Rothwell, D. J. Sharp, Externally induced frontoparietal synchronization modulates network dynamics and enhances working memory performance. *eLife* **6**, e22001 (2017).
8. I. Alekseichuk, Z. Turi, G. Amador de Lara, A. Antal, W. Paulus, Spatial working memory in humans depends on theta and high gamma synchronization in the prefrontal cortex. *Curr. Biol.* **26**, 1513–1521 (2016).
9. B. Cottereau, J. Lorenceau, A. Gramfort, M. Clerc, B. Thirion, S. Baillet, Phase delays within visual cortex shape the response to steady-state visual stimulation. *Neuroimage* **54**, 1919–1929 (2011).
10. A. M. Norcia, L. G. Appelbaum, J. M. Ales, B. R. Cottereau, B. Rossion, The steady-state visual evoked potential in vision research: A review. *J. Vis.* **15**, 4 (2015).
11. K. E. Mathewson, C. Prudhomme, M. Fabiani, D. M. Beck, A. Lleras, G. Gratton, Making waves in the stream of consciousness: Entraining oscillations in EEG alpha and fluctuations in visual awareness with rhythmic visual stimulation. *J. Cogn. Neurosci.* **24**, 2321–2333 (2012).
12. T. A. de Graaf, J. Gross, G. Paterson, T. Rusch, A. T. Sack, G. Thut, Alpha-band rhythms in visual task performance: Phase-locking by rhythmic sensory stimulation. *PLOS ONE* **8**, e60035 (2013).
13. A. M. Cravo, G. Rohenkohl, V. Wyart, A. C. Nobre, Temporal expectation enhances contrast sensitivity by phase entrainment of low-frequency oscillations in visual cortex. *J. Neurosci.* **33**, 4002–4010 (2013).
14. E. Spaak, F. P. de Lange, O. Jensen, Local entrainment of alpha oscillations by visual stimuli causes cyclic modulation of perception. *J. Neurosci.* **34**, 3536–3544 (2014).
15. M. J. Henry, B. Herrmann, J. Obleser, Entrained neural oscillations in multiple frequency bands comodulate behavior. *Proc. Natl. Acad. Sci. U.S.A.* **111**, 14935–14940 (2014).
16. M. J. Henry, J. Obleser, Frequency modulation entrains slow neural oscillations and optimizes human listening behavior. *Proc. Natl. Acad. Sci. U.S.A.* **109**, 20095–20100 (2012).
17. S. Ten Oever, C. E. Schroeder, D. Poeppel, N. van Atteveldt, A. D. Mehta, P. Mégevand, D. M. Groppe, E. Zion-Golumbic, Low-frequency cortical oscillations entrain to subthreshold rhythmic auditory stimuli. *J. Neurosci.* **37**, 4903–4912 (2017).
18. E. B. J. Coffey, I. Arseneau-Bruneau, X. Zhang, S. Baillet, R. J. Zatorre, Oscillatory entrainment of the frequency following response in auditory cortical and subcortical structures. *J. Neurosci.* **41**, 4073–4087 (2021).
19. E. B. Coffey, S. C. Herholz, A. M. Chepesiuk, S. Baillet, R. J. Zatorre, Cortical contributions to the auditory frequency-following response revealed by MEG. *Nat. Commun.* **7**, 11070 (2016).
20. M. Gomez-Ramirez, S. P. Kelly, S. Molholm, P. Sehatpour, T. H. Schwartz, J. J. Foxe, Oscillatory sensory selection mechanisms during intersensory attention to rhythmic auditory and visual inputs: A human electrocorticographic investigation. *J. Neurosci.* **31**, 18556–18567 (2011).
21. J. Duncan, The multiple-demand (MD) system of the primate brain: Mental programs for intelligent behaviour. *Trends Cogn. Sci.* **14**, 172–179 (2010).
22. T. A. Niendam, A. R. Laird, K. L. Ray, Y. M. Dean, D. C. Glahn, C. S. Carter, Meta-analytic evidence for a superordinate cognitive control network subserving diverse executive functions. *Cogn. Affect. Behav. Neurosci.* **12**, 241–268 (2012).
23. N. E. Foster, A. R. Halpern, R. J. Zatorre, Common parietal activation in musical mental transformations across pitch and time. *Neuroimage* **75**, 27–35 (2013).
24. H. Hamada, D. Matsuzawa, C. Sutoh, Y. Hirano, S. Chakraborty, H. Ito, H. Tsuji, T. Obata, E. Shimizu, Comparison of brain activity between motor imagery and mental rotation of the hand tasks: A functional magnetic resonance imaging study. *Brain Imaging Behav.* **12**, 1596–1606 (2018).
25. G. Vingerhoets, F. P. de Lange, P. Vandemaele, K. Deblaere, E. Achten, Motor imagery in mental rotation: An fMRI study. *Neuroimage* **17**, 1623–1633 (2002).
26. O. Jensen, C. D. Tesche, Frontal theta activity in humans increases with memory load in a working memory task. *Eur. J. Neurosci.* **15**, 1395–1399 (2002).
27. W. Klimesch, EEG alpha and theta oscillations reflect cognitive and memory performance: A review and analysis. *Brain Res. Brain Res. Rev.* **29**, 169–195 (1999).
28. P. Sauseng, W. Klimesch, M. Schabus, M. Doppelmayr, Fronto-parietal EEG coherence in theta and upper alpha reflect central executive functions of working memory. *Int. J. Psychophysiol.* **57**, 97–103 (2005).
29. W. Klimesch, R. Freunberger, P. Sauseng, W. Gruber, A short review of slow phase synchronization and memory: Evidence for control processes in different memory systems? *Brain Res.* **1235**, 31–44 (2008).
30. R. N. Shepard, J. Metzler, Mental rotation of three-dimensional objects. *Science* **171**, 701–703 (1971).
31. N. E. Foster, R. J. Zatorre, A role for the intraparietal sulcus in transforming musical pitch information. *Cereb. Cortex* **20**, 1350–1359 (2010).
32. F. Varela, J. P. Lachaux, E. Rodriguez, J. Martinerie, The BrainWeb: Phase synchronization and large-scale integration. *Nat. Rev. Neurosci.* **2**, 229–239 (2001).
33. J. D. Herring, G. Thut, O. Jensen, T. O. Bergmann, Attention modulates TMS-locked alpha oscillations in the visual cortex. *J. Neurosci.* **35**, 14435–14447 (2015).
34. P. Sauseng, B. Griesmayr, R. Freunberger, W. Klimesch, Control mechanisms in working memory: A possible function of EEG theta oscillations. *Neurosci. Biobehav. Rev.* **34**, 1015–1022 (2010).
35. J. Lisman, Working memory: The importance of theta and gamma oscillations. *Curr. Biol.* **20**, R490–R492 (2010).
36. J. Fell, N. Axmacher, The role of phase synchronization in memory processes. *Nat. Rev. Neurosci.* **12**, 105–118 (2011).
37. A. Baddeley, Working memory. *Curr. Biol.* **20**, R136–R140 (2010).
38. C. Wendelken, S. A. Bunge, C. S. Carter, Maintaining structured information: An investigation into functions of parietal and lateral prefrontal cortices. *Neuropsychologia* **46**, 665–678 (2008).
39. M. D'Esposito, From cognitive to neural models of working memory. *Philos. Trans. R. Soc. Lond. B Biol. Sci.* **362**, 761–772 (2007).
40. B. R. Postle, J. S. Berger, M. D'Esposito, Functional neuroanatomical double dissociation of mnemonic and executive control processes contributing to working memory performance. *Proc. Natl. Acad. Sci. U.S.A.* **96**, 12959–12964 (1999).
41. J. Jonides, E. H. Schumacher, E. E. Smith, R. A. Koeppe, E. Awh, P. A. Reuter-Lorenz, C. Marshuetz, C. R. Willis, The role of parietal cortex in verbal working memory. *J. Neurosci.* **18**, 5026–5034 (1998).

42. A. S. Champod, M. Petrides, Dissociation within the frontoparietal network in verbal working memory: A parametric functional magnetic resonance imaging study. *J. Neurosci.* **30**, 3849–3856 (2010).
43. A. S. Champod, M. Petrides, Dissociable roles of the posterior parietal and the prefrontal cortex in manipulation and monitoring processes. *Proc. Natl. Acad. Sci. U.S.A.* **104**, 14837–14842 (2007).
44. J. Duncan, A. M. Owen, Common regions of the human frontal lobe recruited by diverse cognitive demands. *Trends Neurosci.* **23**, 475–483 (2000).
45. E. K. Miller, J. D. Cohen, An integrative theory of prefrontal cortex function. *Annu. Rev. Neurosci.* **24**, 167–202 (2001).
46. F. Tadel, S. Baillet, J. C. Mosher, D. Pantazis, R. M. Leahy, Brainstorm: A user-friendly application for MEG/EEG analysis. *Comput. Intell. Neurosci.* **2011**, 879716 (2011).
47. J. Gross, S. Baillet, G. R. Barnes, R. N. Henson, A. Hillebrand, O. Jensen, K. Jerbi, V. Litvak, B. Maess, R. Oostenveld, L. Parkkonen, J. R. Taylor, V. van Wassenhove, M. Wibral, J. M. Schoffelen, Good practice for conducting and reporting MEG research. *Neuroimage* **65**, 349–363 (2013).
48. C. Tallon-Baudry, O. Bertrand, Oscillatory gamma activity in humans and its role in object representation. *Trends Cogn. Sci.* **3**, 151–162 (1999).

Acknowledgments: We thank J. Kweon and D. Fu for their contribution in data collection. **Funding:** This work was supported by a CIHR Foundation grant to R.J.Z.; by NSERC Discovery grants to P.A., S.B., and R.J.Z.; and by two grants to S.B. and R.J.Z. from the Healthy Brains for Healthy Lives initiative of McGill University under the Canada First Research Excellence Fund. P.A. was funded by an NSERC Banting Fellowship. R.J.Z. is a fellow of the Canadian Institute for Advanced Research and is funded via the Canada Research Chair Program. S.B. is also supported by the CIHR Canada Research Chair of Neural Dynamics of Brain Systems and the NIH (1R01EB026299). P.A. is supported by FRQS Junior 1 grant. **Author contributions:** Conceptualization: P.A., S.B., and R.J.Z. Methodology: P.A., R.J.Z., and S.B. Analysis: P.A. Investigation: P.A., R.S.H., and Z.E.M.-M. Resources: P.A., R.J.Z., and S.B. Writing—original draft: P.A. Writing—review and editing: P.A., Z.E.M.-M., R.S.H., S.B., and R.J.Z. Visualization: P.A. Supervision: P.A., R.J.Z., and S.B. Project administration: P.A., R.J.Z., and S.B. **Competing interests:** The authors declare that they have no competing interests. **Data and materials availability:** Behavioral and EEG data are freely available at https://osf.io/4ck59/.

Submitted 14 June 2021
Accepted 29 December 2021
Published 23 February 2022
10.1126/sciadv.abj9782